

# Immunohistochemical profiling of caspase signaling pathways predicts clinical response to chemotherapy in primary nodal diffuse large B-cell lymphomas

Jettie J. F. Muris, Saskia A. G. M. Cillessen, Wim Vos, Inge S. van Houdt, J. Alain Kummer, Johan H. J. M. van Krieken, N. Mehdi Jiwa, Patty M. Jansen, Hanneke C. Kluin-Nelemans, Gert J. Ossenkoppele, Chad Gundy, Chris J. L. M. Meijer, and Joost J. Oudejans

**We used biopsy specimens of primary nodal diffuse large B-cell lymphoma (DLBCL) to investigate whether the inhibition of caspase 8 and/or 9 apoptosis signaling pathways predicts clinical outcome. Expression levels of cellular FLICE inhibitory protein (c-Flip) and numbers of active caspase 3–positive lymphoma cells were used to determine the status of the caspase 8–mediated pathway. Expression levels of Bcl-2 and X-linked inhibitor of apoptosis (XIAP) were used to deter-**

**mine the status of the caspase 9–mediated pathway. Expression of c-Flip, XIAP, Bcl-2, and caspase 3 activity all provided prognostic information. According to these immunohistochemical parameters, inhibition of either or both caspase signaling pathways was detected in all patients. Three groups of patients were identified, one with a caspase 8 inhibition profile, one with caspase 8 and 9 inhibition profiles, and one with a caspase 9 inhibition profile. Caspase 9 inhibition was strongly**

**associated with poor response to chemotherapy and usually with fatal outcome, whereas caspase 8 inhibition was associated with excellent clinical outcome. Thus, our data strongly suggest that inhibition of the caspase 9–mediated pathway, but not the caspase 8–mediated pathway, is a major cause for therapy resistance in patients with nodal DLBCL. (Blood. 2005; 105:2916-2923)**

© 2005 by The American Society of Hematology

## Introduction

Diffuse large B-cell lymphomas (DLBCLs) are the most frequent type of non-Hodgkin lymphoma (NHL) and account for 40% of adult NHL.<sup>1</sup> DLBCLs are potentially curable with multiagent chemotherapy, but the disease proves fatal in approximately 50% of patients. The International Prognostic Index (IPI) is used to categorize patients into low- and high-risk groups.<sup>2</sup> Still, clinical outcome in the individual patient remains unpredictable. It is probable that in patients with fatal outcomes, the tumor cells are intrinsically resistant to chemotherapy-induced cell death because chemotherapy fails to induce complete tumor remission in most of them.

Many studies have shown that the cell death–inducing effect of chemotherapy depends on the induction of apoptosis and that disruption of the apoptosis signaling cascade may thus be an important cause for chemotherapy resistance.<sup>3,4</sup> Two major apoptosis pathways have been described,<sup>5</sup> a stress-induced caspase 9–mediated pathway and a death receptor–induced caspase 8–mediated pathway (Figure 1).<sup>6,7</sup> The stress-induced pathway is activated by p53 after DNA damage and is preferentially involved in chemotherapy-induced cell death.<sup>8</sup> The stress-induced pathway can be inhibited at many levels. The most potent inhibitors of this pathway appear to be Bcl-2 and the X-linked inhibitor of apoptosis (XIAP).<sup>5,9-11</sup>

The caspase 8–mediated pathway can be triggered by ligation of specific death receptors by FAS ligand, tumor necrosis factor- $\alpha$  (TNF- $\alpha$ ), and TNF-related apoptosis-inducing ligand (TRAIL),

also known as Apo2 ligand (Apo2L). In addition, spontaneous apoptosis observed during the follicle center cell reaction is primarily mediated by caspase 8 activation.<sup>12,13</sup> An important regulator of this pathway is cellular FLICE inhibitory protein (c-Flip).<sup>14-17</sup> Expression of c-Flip was previously detected in Hodgkin and Reed-Sternberg cells in almost all Hodgkin lymphoma biopsy specimens.<sup>18,19</sup>

Both pathways induce apoptosis by the activation of caspase 3 and possibly other effector caspases. We have previously demonstrated that apoptosis in B-cell lymphomas indeed always involves the activation of caspase 3.<sup>20</sup>

In this study we investigated whether the inhibition of caspase 8– or caspase 9–, or both, mediated apoptosis signaling pathways is related to clinical response to chemotherapy and to eventual clinical outcome in patients with primary nodal DLBCL. To determine the status of the caspase 8–mediated pathway, c-Flip expression and caspase 3 and caspase 8 activation levels were used, whereas the status of the caspase 9–mediated pathway was determined by expression levels of Bcl-2 and XIAP.

Furthermore, we investigated whether differences in these immunohistochemically determined apoptosis profiles were related to clinical characteristics included in the IPI and to the recently described germinal center B cell–like (GCB) versus non–GCB–like phenotype.<sup>21-23</sup>

From the Departments of Clinical Pathology, Haematology, and Clinical Epidemiology and Biostatistics, VU Medical Center; the Department of Clinical Pathology, Utrecht Medical Center; the Department of Clinical Pathology, Radboud University Medical Center; the Department of Clinical Pathology Medical Center Alkmaar; the Department of Clinical Pathology, Leiden University Medical Centre; and the Department of Hematology, University Hospital Groningen, The Netherlands.

Submitted July 16, 2004; accepted November 26, 2004. Prepublished online as *Blood* First Edition Paper, December 2, 2004; DOI 10.1182/blood-2004-07-2716.

Supported by the Dutch Cancer Foundation (grant VU 2003-2818).

**Reprints:** J.J. Oudejans, Department of Clinical Pathology, VU Medical Center, De Boelelaan 1117, 1007 MB Amsterdam, The Netherlands; e-mail: jj.oudejans@vumc.nl.

The publication costs of this article were defrayed in part by page charge payment. Therefore, and solely to indicate this fact, this article is hereby marked “advertisement” in accordance with 18 U.S.C. section 1734.

© 2005 by The American Society of Hematology

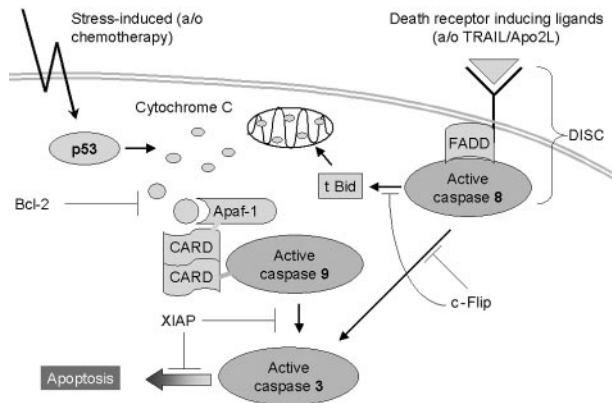


**Figure 1. Schematic representation of both major apoptosis signaling pathways.** Chemotherapy causes DNA damage, inducing p53-controlled cytochrome *c* release from mitochondria, which then binds to apoptosis-activating factor-1 (Apaf-1), resulting in the activation of caspase 9, followed by the activation of effector caspases including caspase 3. Bcl-2 inhibits apoptosis at the level of cytochrome *c* release, whereas XIAP exerts its antiapoptotic effect through interaction with active caspase 9 and with active caspase 3.<sup>6</sup> After ligation, death receptors signal cell death by inducing a death-inducing signaling complex (DISC) composed of the cytoplasmic adapter protein Fas-associated death domain (FADD) and caspase 8. Activated caspase 8 can activate caspase 3 directly and indirectly by the truncation of Bid. The truncated form of Bid (t Bid) translocates to mitochondria leading to cytochrome *c* release and activation of the caspase 9–mediated pathway. c-Flip inhibits caspase 8 activation by interfering with the recruitment and the processing of pro-caspases within the DISC.<sup>7</sup>

## Patients, materials, and methods

### Patient selection and clinical characteristics

Patients with primary nodal DLBCL ( $n = 80$ ) were selected from the files of the Comprehensive Cancer Center Amsterdam (diagnosed between 1986 and 1998), the Department of Pathology of the University Hospital Nijmegen (diagnosed between 1991 and 1999), and the Department of Pathology of the Leiden University Medical Center (diagnosed between 1991 and 2000), The Netherlands. The only selection criteria were availability of paraffin-embedded material and clinical follow-up data. Patients were reclassified according to the World Health Organization (WHO) classification.<sup>24</sup> To include only patients with primary nodal DLBCL, those with extranodal disease (localized stage IE or IIE disease) were excluded.<sup>25</sup> At first presentation, the extent of the disease was determined through physical examination, serum lactate dehydrogenase (LDH) concentration, full blood count, bone marrow aspirate and biopsy, chest x-ray, and computed tomography of chest, abdomen, and pelvis. From the medical records, the following characteristics were noted: age at diagnosis, sex, Ann Arbor stage at presentation, therapy, achievement of complete remission, occurrence of relapses, and cause of death. The International Prognostic Index (IPI) score was determined, as described previously.<sup>2</sup> The institutional review board of the VU Medical Center approved the study. Informed consent was provided according to the Declaration of Helsinki.

### Detection of pro-caspase 3 and active caspase 3, cleaved PARP-1/p89, active caspase 8, c-Flip, Bcl-2, XIAP, CD-10, Bcl-6, and MUM1

**Immunohistochemistry.** Three-micrometer-thick sections from the paraffin-embedded biopsy specimens were stained with the following antibodies: polyclonal rabbit antiactive caspase 3, polyclonal rabbit antiactive caspase 8 (both Cell Signaling Technology, Beverly, MA), monoclonal mouse anti-c-Flip (clone NF6; Alexis, Lausen, Switzerland), mouse anti-Bcl-2 (clone 124; DakoCytomation, Glostrup, Denmark), mouse anti-XIAP (clone 2F1; MBL, Nagoya, Japan), mouse anti-CD10 (clone 56C6; Monosan, Uden, The Netherlands), mouse anti-Bcl-6 (clone PG-B6p;

DakoCytomation), and mouse anti-MUM1 (clone MUM1p; DakoCytomation). For pro-caspase 3, the polyclonal rabbit anti-pro-caspase 3 (CPP32; DakoCytomation) was used, and the polyclonal rabbit anti-p89 (Promega, Madison, WI) was used to detect the cleaved fragment form of PARP-1.<sup>26,27</sup>

Antibodies required antigen retrieval in citrate buffer (10 mM, pH 6.0) for pro-caspase 3, active caspase 3, Bcl-2, XIAP, and Bcl-6. Antigen retrieval in Tris EDTA (ethylenediaminetetraacetic acid) buffer (10 mM/1 mM, pH 9.0) was required for p89, c-Flip, CD10, and MUM1. After antigen retrieval, antibodies were incubated for 1 hour at room temperature or were incubated overnight (active caspase 3, c-Flip, Bcl-2, and XIAP). The catalyzed reported deposition (CARD) method (DakoCytomation) was used to detect pro-caspase 3 and Bcl-2. For active caspase 3, p89, active caspase 8, c-Flip, XIAP, CD10, Bcl-6, and MUM1, a standard, highly sensitive EnVision horseradish peroxidase system (DakoCytomation) was used. Visualizations were performed using diaminobenzidine (DAB) as chromogen. Nonneoplastic lymphoid tissues served as positive control for all tested antibodies. For c-Flip detection, 5 classical Hodgkin lymphomas were also included as positive controls.

**Double-staining procedures.** To determine whether active caspase 3 and PARP-1/p89–positive cells in DLBCL are indeed neoplastic cells, double stainings were performed in 5 patients for active caspase 3 and CD20 and for PARP-1/p89 and CD20. Antibodies against active caspase 3 and PARP-1/p89 were rabbit antibodies mixed with mouse anti-CD20 antibody (clone L26, mouse IgG<sub>2a</sub>; DakoCytomation) in appropriate concentrations and were incubated for 1 hour. Both secondary antibodies—biotinylated polyclonal donkey-antirabbit (Jackson ImmunoResearch Laboratories, West Grove, PA) and alkaline phosphatase–labeled goat antimouse IgG<sub>2a</sub> (Southern Biotechnology, Birmingham, AL)—were mixed and incubated for 30 minutes. Active caspase 3 and PARP-1/p89 were detected after amplification with the sensitive CARD method (DakoCytomation). Active caspase 3– and PARP-1/p89–positive staining were visualized with DAB. CD20<sup>+</sup> staining was visualized with naphthol as MX phosphate and fast-blue BB phosphate. Negative controls included simultaneously processed slides with omission of the primary antibodies. Images were obtained using a Leica DM 4000 B microscope equipped with a 63 ×/0.75 objective lens and a Leica DC 500 digital imaging system. Postprocessing and white balancing were done with Adobe Photoshop 7.0 (San Jose, CA).

**Quantification of active caspase 3– and cleaved PARP-1/p89–positive cells.** Percentages of active caspase 3– and cleaved PARP-1/p89–positive tumor cells were quantified using a commercially available interactive video overlay–based measuring system (Q-PROFIT; Leica, Cambridge, United Kingdom), as described previously.<sup>28,29</sup> In the selected areas, up to 150 fields of vision were screened, and within these fields at least 75 to 100 tumor cells were counted. To avoid counting macrophages with phagocytosed apoptotic debris, only cells with nuclear staining or with nuclear and cytoplasmic staining were counted.

**Quantification of c-Flip, Bcl-2, XIAP, and pro-caspase 3.** c-Flip, Bcl-2, XIAP, and pro-caspase 3–positive tumor cells were evaluated semiquantitatively as percentages of all tumor cells. For Bcl-2, XIAP, and pro-caspase 3, reactive lymphocytes served as internal positive control. For c-Flip expression, endothelial cells served as an internal positive control while GCB cells in hyperplastic tonsils served as an external positive control.<sup>18</sup> All stainings were analyzed independently by 2 observers. If they disagreed, the observers reanalyzed the staining results until they reached a consensus.

**Functional analysis of sensitivity to chemotherapy-induced apoptosis.** Sensitivity to chemotherapy-induced apoptosis was performed as described elsewhere (S.A.G.M.C., C.J.L.M.M., Kitty C. M. Castricum, Petra Niesten, J.J.F.M., G.J.O., W.V., Marcel J. Flens, and J.J.O., manuscript in preparation). Briefly, isolated lymphoma cells of 6 prospectively collected DLBCL samples were incubated for 4 hours with 25 μM etoposide (VP16; Sigma, St Louis, MO) after negative selection using superparamagnetic Dynabeads coated with CD3 antibodies (Dyna, Wirral, United Kingdom). Caspase 3–like effector caspase activity was determined in isolated lymphoma cells using a fluorometric homogeneous caspase assay (Roche, Mannheim, Germany), according to the manufacturer's instructions in 1E5 cells. Sensitivity to etoposide-induced apoptosis was determined as the ratio

between etoposide-induced caspase activation and untreated samples. Experiments were performed in triplicate.

**Classification in GCB or non-GCB subtypes according to expression of CD10, Bcl-6, and MUM1.** Patients were categorized as GCB or non-GCB cell subtype according to the algorithm recently published by Hans et al<sup>23</sup> using the same cut-off values for the different markers. Briefly, patients were assigned to the GCB group if CD10 alone or if both CD10 and Bcl-6 were positive. If both CD10 and Bcl-6 were negative, the patient was assigned to the non-GCB subgroup. In the remaining Bcl-6-positive, CD10-negative patients, expression of MUM1 determined GCB phenotype. MUM1-negative patients were assigned to the GCB subgroup, and MUM1-positive patients were assigned to the non-GCB subgroup.

### Analysis of clinical data

Survival time was measured from time of initial diagnosis until death, with or without disease, or until the end of follow-up. Analysis of disease-free survival time was performed only for patients who achieved complete remission and was measured from time of initial diagnosis until diagnosis of relapse.

Survival curves were constructed according to the Kaplan-Meier method. Differences between the curves were analyzed using the log-rank test. Multivariate analysis for overall survival time was performed using the Cox proportional hazards model.<sup>30</sup> Multivariate analysis for the chance to reach complete remission was performed by log linear regression analysis using the Wald test. Qualitative variables were analyzed by the Pearson  $\chi^2$  test or by the Fisher exact test, when appropriate. The Kruskal-Wallis test was used to compare group means, and the Spearman test was used to test correlations between different variables. All *P* values were based on 2-tailed statistical analysis, with *P* < .05 considered significant. Analyses were performed using SPSS statistical software (version 10.1; SPSS Inc, Chicago, IL). The optimal cut-off value for the percentage of active caspase 3-, p89, Bcl-2-, and XIAP-positive tumor cells was determined using 2 methods: (1) log-rank test, testing the prognostic value for each possible cut-off point (eg, 1%, 2%, 3%) for active caspase 3 and p89 and (eg, 10%, 20%, 30%) for c-Flip, Bcl-2 and XIAP; and (2) Cox regression analysis, including all points as categorical variables. Both methods gave identical results.

## Results

### Patient characteristics

Clinical data were available for all patients and are summarized in Table 1. For 1 patient, the data concerning stage and, therefore, IPI could not be retrieved. Age distribution showed a peak in the seventh decade, with a slightly male predominance; approximately

**Table 1. Clinical characteristics**

Characteristic	No. of patients, N = 80
Median age, y (range)	62 (14-94)
Sex, M/F	48/32
<b>Stage (%)*</b>	
1 + 2	34 (43)
3 + 4	45 (57)
B symptoms	26 (33)
<b>IPI (%)*</b>	
Low/low-intermediate	45 (57)
Intermediate-high/high	34 (43)
<b>Therapy</b>	
CHOP-like	47
CHOP-like + RT	33
Complete remission (%)	54 (68)
Relapse (%)	19 (35)
Death (%)	46 (57)

RT indicates radiotherapy.

\*Data concerning stage and IPI could not be retrieved for 1 patient.

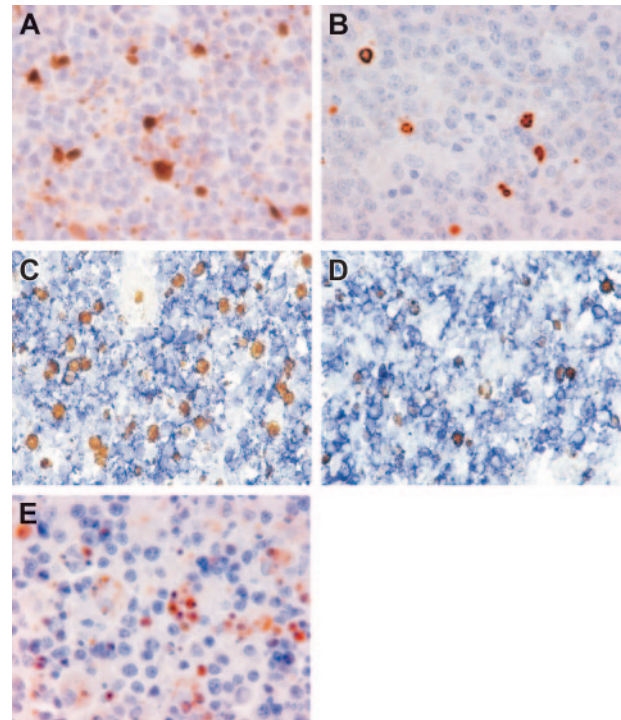


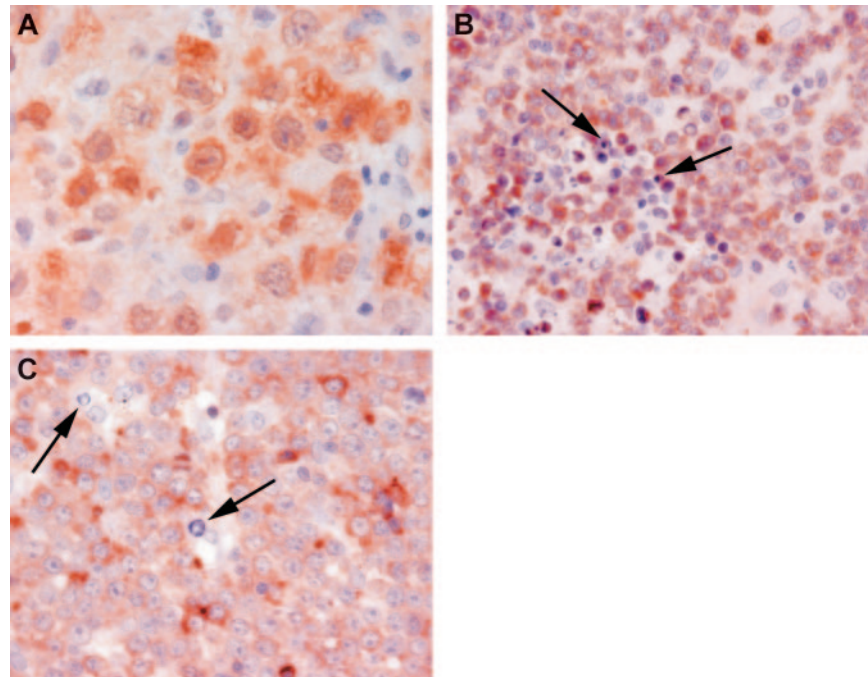
**Figure 2. Detection of active caspase 3 and cleaved PARP-1/p89 in biopsy specimens of primary nodal DLBCL.** (A) Staining for active caspase 3 demonstrating brown, mostly nuclear, staining primarily in cells with morphologic features of apoptosis. (B) Cleaved PARP-1/p89 staining demonstrated strictly nuclear staining, also primarily in cells with morphologic features of apoptosis. (C) Double staining for active caspase 3 and CD20. (D) Cleaved PARP-1/p89 and CD20 demonstrating that active caspase 3-positive cells and cleaved PARP-1/p89-positive cells (both brown nuclear staining) are CD20+ positive (blue membranous staining) and thus probably neoplastic B cells. (E) Staining for active caspase 8 demonstrating brown, mostly nuclear, staining, also primarily in cells with morphologic features of apoptosis.

half of all patients presented with advanced disease, in line with other studies.<sup>1,31</sup> All patients were treated according to standard primary anthracycline-containing combination chemotherapy (predominantly cyclophosphamide, hydroxydaunomycin/doxorubicin, Oncovin, prednisone [CHOP]), either alone or in combination with involved field irradiation (n = 47 and n = 33, respectively); 54 of 80 patients achieved complete remission. Of these 54 patients, 19 (35%) experienced relapse, with a median disease-free survival time of 25 months (range, 4 to 118 months). IPI score was a strong prognostic marker (*P* = .003), consistent with previous studies.<sup>2</sup>

### Spontaneous caspase 3 activity correlates with PARP-1 cleavage and caspase 8 activation and varies strongly among lymphomas

In all patients tested (n = 80), active caspase 3-positive cells were observed, displaying a mainly nuclear staining pattern usually in cells with morphologic features of apoptosis (Figure 2A). The percentage of active caspase 3-positive tumor cells ranged from less than 1% to 17%, with a median of 3.5%. As in our previous study,<sup>20</sup> the number of active caspase 3-positive tumor cells correlated strongly with the number of PARP-1/p89-positive tumor cells (Spearman correlation, *R* = 0.87; *P* < .001), suggesting proper functioning of active caspase 3 (Figure 2B). Using double-staining procedures, we found in all patients tested (n = 5) that staining for active caspase 3 and PARP-1/p89 was largely restricted to CD20+ tumor cells (Figure 2C-D). To investigate whether caspase 3 activation correlates with caspase 8 activation, we stained for active caspase 8- in 10 patients with high numbers of active caspase 3 and in 10 patients with low numbers of active caspase

**Figure 3. Detection of apoptosis-regulating proteins in biopsy specimens of primary nodal DLBCL.** (A) c-Flip demonstrating brown, predominantly cytoplasmic, staining. (B) Bcl-2 demonstrating brown cytoplasmic staining. (C) XIAP demonstrating brown cytoplasmic staining. Arrows indicate apoptotic cells. Note high numbers of cells with apoptotic morphology in clearly Bcl-2- and XIAP-positive patients and the absence of cells with apoptotic morphology in c-Flip-positive patients.



8-positive cells. Although slightly less intense, the staining was highly comparable to that of active caspase 3-positive cells in all patients, demonstrating primarily nuclear staining in cells with apoptotic morphology (Figure 2E). In all tested patients (n = 20), numbers of active caspase 8-positive cells were similar to the numbers of active caspase 3- and PARP-1/p89-positive cells.

**Expression of c-Flip, Bcl-2, XIAP, and pro-caspase 3**

c-Flip expression was found in 24 of 69 (35%) patients with interpretable data. In positive patients, c-Flip expression was detected as cytoplasmic staining in a maximum of 30% of the neoplastic cells (Figure 3A). In addition, Bcl-2 and XIAP were detected as cytoplasmic staining (Figure 3B-C). Bcl-2 expression was detected in 63 of 79 patients with interpretable data. In positive patients, the percentage of Bcl-2-positive tumor cells ranged from 5% to 100%; the median was 80%. XIAP expression was observed as granular cytoplasmic staining in 49 of 73 patients with interpretable data. In positive patients, the percentage of XIAP-positive tumor cells ranged from 10% to 100%; the median was 20%. Pro-caspase 3 was detected in all patients with DLBCL, consistent with previous studies.<sup>20,32</sup>

**Survival analysis of active caspase 3, c-Flip, Bcl-2, and XIAP**

When tested individually, all 4 markers demonstrated prognostic value, as determined by the log-rank test for prediction of overall survival time and by the  $\chi^2$  test for the chance to reach complete remission (Table 2). In addition, Cox regression analysis was used to determine the prognostic value of percentages of active caspase 3-positive tumor cells when entered as a continuous variable. Using this method, we found that the prognosis declined with increasing percentages of active caspase 3-positive cells (P = .01). The threshold giving the greatest discriminative power was found to be 5%. For c-Flip, the threshold with the greatest discriminative power was found when patients were considered negative or positive, irrespective of the number of positive cells. Using log-rank and Cox regression analyses, the threshold with the

greatest discriminative value for Bcl-2 and XIAP was found to be 50%. The prognostic value of percentages of active caspase 3-positive cells, c-Flip, Bcl-2, and XIAP expression were independent of the IPI score and of the GCB profile. Multivariate regression analysis using the Wald test showed that the percentage of active caspase 3-positive cells and Bcl-2 expression remained independent prognostic predictors for the chance to reach complete remission.

**Patients with high percentages of active caspase 3-positive cells are c-Flip negative and express Bcl-2, XIAP, or both**

A strong relation between percentages of active caspase 3-positive cells and expression of apoptosis-inhibiting proteins was observed (Table 3). Expression of c-Flip was predominantly found in

**Table 2. Univariate survival analysis of apoptosis-related proteins**

Characteristic	N	Complete remission, %	P*	5-y survival	P†
<b>Active caspase 3</b>					
Low, less than 5%	53	83	.001	50	.0001
High, more than 5%	27	38		20	
NI	0	—		—	
<b>c-Flip</b>					
Negative	45	63	.03	30	.03
Positive	24	83		55	
NI	11	—		—	
<b>Bcl-2</b>					
Negative, less than 50%	16	94	.008	85	.001
Positive, more than 50%	63	60		30	
NI	1	—		—	
<b>XIAP</b>					
Negative, less than 50%	49	69	NS	50	.02
Positive, more than 50%	24	67		25	
NI	7	—		—	

NI indicates not interpretable; NS, not significant.  
 \*As determined by the Fisher exact test.  
 †As determined by the log rank test.

**Table 3. Expression of apoptosis-regulating proteins in relation to percentages of active caspase 3–positive tumor cells**

	Active caspase 3–positive tumor cells, %		P*
	Less than 5% n = 53	At least 5% n = 27	
<b>c-Flip</b>			
Negative	26	19	.01
Positive	21	3	
NI	6	5	
<b>Bcl-2</b>			
Negative, less than 50%	13	3	NS
Positive, more than 50%	39	24	
NI	1	0	
<b>XIAP</b>			
Negative, less than 50%	38	11	.03
Positive, more than 50%	12	12	
NI	3	4	
<b>Bcl-2-XIAP</b>			
Both negative	11	0	.01
One or both positive	42	27	
NI	0	0	

NI indicates not interpretable.

\*As determined by the Fisher exact test.

patients with few active caspase 3–positive tumor cells.<sup>3</sup> In contrast, patients with high percentages of caspase 3 activation always expressed Bcl-2 or XIAP, or both (Table 3). Based on these results, patients were divided into 3 groups (Table 4). Because caspase 3 activity closely correlated with caspase 8 activity, all patients with low numbers of active caspase 3–positive tumor cells were assigned a caspase 8 inhibition profile, including lymphomas, without expression of c-Flip (n = 26).

#### Inhibition of apoptosis-mediated pathways is a frequent event and strongly predicts response to chemotherapy and clinical outcome

When patients were divided according to the immunohistochemical apoptosis profile in the 3 groups described in Table 4, strong differences in clinical outcome were observed (Table 5; Figure 4). Patients with the caspase 8 inhibition profile always achieved complete remission. Only 1 patient experienced relapse, and none of the patients died. This is in contrast to the group of patients with the caspase 9 inhibition profile. Only 9 of 24 patients achieved complete remission, and 19 patients died within 3 years of diagnosis. Unexpectedly, patients with immunohistochemical evidence of inhibition of both pathways fared significantly better than did patients with only caspase 9 inhibition (log-rank test,  $P = .01$ ). Most of these patients achieved complete remission but then experienced relapse, usually with fatal outcome. Thus, grouping according to immunohistochemical apoptosis profile strongly predicted the chance to achieve complete remission ( $\chi^2$  test,  $P < .001$ ) and overall survival time (log-rank test,  $P < .0001$ ). Patients with the caspase 9 inhibition profile also tended to experience relapse more frequently than did patients without this profile. Apoptosis profile was not related to IPI score (Table 5) and did retain its prognostic power for low/low-intermediate and intermediate-high/high IPI groups, respectively (Figure 5A-B). However, in patients with low/low-intermediate IPI scores, no difference was found between those with inhibition of both pathways and those with inhibition of only the caspase 9–mediated pathway.

#### Immunohistochemical apoptosis profiling correlates with in vitro–determined sensitivity to etoposide-induced apoptosis

To investigate whether the immunohistochemical apoptosis profile correlates with functional sensitivity to chemotherapy-induced apoptosis, we tested 6 prospectively selected patients with DLBCL. Indeed, the highest levels of etoposide-induced caspase 3 activation were observed in the 2 patients without immunohistochemical evidence of caspase 9 inhibition (Table 6). Moreover, high levels of etoposide-induced caspase activation correlated with the achievement of complete remission.

#### Predictive power of GCB versus non-GCB immune phenotype is partly explained by association with inhibition of the caspase 9–mediated pathway

Immunohistochemical analysis for CD10, Bcl-6, and MUM1 was performed in 68 patients to determine a GCB or a non-GCB profile. GCB phenotype was detected in 37% of patients; patients with GCB profiles fared significantly better than those with non-GCB profiles ( $P = .02$ ). When the GCB profile was compared with the apoptosis profile, it appeared that the non-GCB profile demonstrated inhibition of the caspase 9 pathway more frequently than the GCB profile (Table 7;  $P = .05$ ). Multivariate analysis for overall survival time, including IPI, apoptosis profile, and GCB profile, identified apoptosis profile as the strongest prognostic marker. IPI score and GCB profile did not add significant prognostic information.

## Discussion

In this study, we have shown that expression profiles of apoptosis-inhibiting proteins have different effects on clinical outcome in patients with DLBCL. Low percentages of active caspase 3–positive tumor cells and expression of c-Flip are related to favorable outcomes, whereas expression of Bcl-2 and XIAP are strongly related to unfavorable outcomes. When all results were included in 1 model (Figure 1), we found that a caspase 8 inhibition profile predicted a highly favorable clinical outcome whereas a caspase 9 inhibition profile was strongly predictive of poor response to chemotherapy and overall survival time. In multivariate analysis, the prognostic power of the apoptosis profile was independent of and stronger than the prognostic power of the IPI score and the GCB profile.

DLBCL originates from GCB cells<sup>12</sup> that normally undergo spontaneous caspase 8–mediated apoptosis in the absence of high-affinity B-cell receptors.<sup>12,13</sup> Inhibition of spontaneous apoptosis in these GCB cells depends on continuous expression of c-Flip.<sup>14–17</sup> Because antigenic stimulation is not necessary to sustain tumor growth in DLBCL, inhibition of the caspase 8–mediated pathway by c-Flip would provide these cells with a strong

**Table 4. Grouping of patients according to apoptosis profile**

No. patients	Caspase 3 activity	c-Flip	Bcl-2/XIAP	Apoptosis profile, inhibition
11	Low	+/-	-	Only caspase 8
45	Low	+/-*	+	Caspases 8 and 9
24	High	-	+	Only caspase 9

\*Three patients with c-Flip expression and with more than 5% active caspase 3–positive lymphoma cells were included.

**Table 5. Patient characteristics in relation to apoptosis profile**

Characteristic	Apoptosis profile			P*
	Caspase 8 inhibition n = 11	Caspase 8 and 9 inhibition n = 45	Caspase 9 inhibition n = 24	
Median age, y (range)	62 (47-70)	63 (14-82)	60 (26-94)	NS§
<b>Sex</b>				
Male	7	24	17	NS
Female	4	21	7	
<b>Stage†</b>				
1 + 2	6	16	12	NS
3 + 4	5	29	11	
<b>B symptoms</b>				
Yes	0	17	9	.05
No	11	28	15	
<b>IPI†</b>				
Low/low-intermediate	7	23	15	NS
Intermediate-high/high	4	22	8	
<b>Therapy</b>				
CHOP-like	5	26	16	NS
CHOP-like + RT	6	19	8	
<b>Complete remission</b>				
Yes	11	34	9	Less than .001
No	0	11	15	
<b>Relapse‡</b>				
Yes	1	15	3	NS
No	10	19	6	
<b>Death</b>				
Yes	0	27	19	Less than .001
No	11	18	5	

RT indicates radiotherapy; NS, not significant.  
 \*As determined by Fisher exact test, unless stated otherwise.  
 †Data concerning stage and IPI could not be retrieved for 1 patient.  
 ‡Patients in relapse were those who did reach complete remission.  
 §As determined by Mann-Whitney U test.

growth advantage. Indeed we found that patients with c-Flip-positivity demonstrated low levels of spontaneous caspase 3 and caspase 8 activation. None of the commercially available c-FLIP antibodies allowed discrimination between the long and short splice forms of c-FLIP, which is important given that c-FLIP<sub>S</sub> exerts an apoptosis inhibitory signal whereas c-FLIP<sub>L</sub> expression may exert proapoptotic and antiapoptotic effects.<sup>33,34</sup> However, Mathas et al<sup>19</sup> demonstrated that the c-FLIP expression detected in

Hodgkin lymphoma does result in the inhibition of caspase 8-mediated apoptosis. Moreover, the strong correlation we observed between c-Flip expression and low levels of caspase 3 and caspase 8 activation suggested that in DLBCL c-Flip expression results in the inhibition, not the induction, of caspase 8-mediated apoptosis. Apparently, inhibition of only this caspase 8-mediated pathway does not interfere with chemotherapy-induced cell death because patients respond favorably to chemotherapy. This is consistent with the notion that chemotherapy-induced cell death involves primarily the caspase 9-mediated pathway.<sup>9</sup>

Our findings that the caspase 9 inhibition profile in DLBCL is strongly associated with a poor response to therapy provide further proof for this notion. Expression of Bcl-2 has previously been

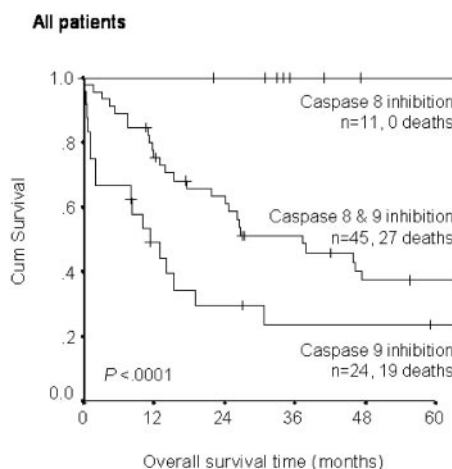


**Figure 4. Comparison of overall survival time in patients with primary nodal DLBCL according to apoptosis profile.** The difference between both lower curves was also significant (log rank test,  $P = .01$ ).

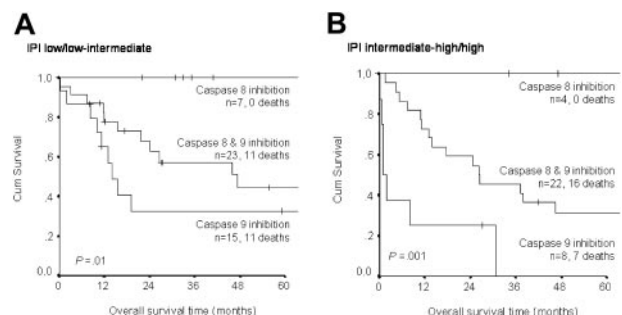


**Figure 5. Comparison of overall survival time in patients with primary nodal DLBCL according to apoptosis profiles for IPI low/low-intermediate and IPI intermediate-high/high.**

**Table 6. In vitro-determined etoposide-induced caspase 3 activation in relation to immunohistochemical apoptosis profile**

Patient	Mean etoposide-induced caspase 3 activity ratio (SD)	Caspase 8 inhibition profile	Caspase 9 inhibition profile	Clinical complete remission
1	2.2 (0.02)	Yes	No	Yes
2	1.8 (0.10)	Yes	No	Yes
3	1.8 (0.03)	Yes	Yes	Yes
4	1.7 (0.02)	Yes	No	Yes
5	1.5 (0.03)	No	Yes	No
6	1.4 (0.02)	No	Yes	No

A high ratio indicates relative strong sensitivity to etoposide-induced caspase 3 activation.

linked to poor prognosis in DLBCL patients.<sup>35-37</sup> The percentage Bcl-2-positive cases was relatively high compared with the study by Barrans et al,<sup>36</sup> who used the same cut-off value for Bcl-2 we used. In the studies by Hermine et al<sup>35</sup> and Kramer et al,<sup>37</sup> DLBCLs were grouped in 3 Bcl-2-expressing categories, making their data more difficult to compare with our data. However, in all these studies, Bcl-2 expression provided strong IPI-independent prognostic information, similar to our results. In addition, we have shown for the first time that the expression of XIAP, reported in several types of lymphoma and lymphoma cell lines,<sup>38-41</sup> is related to poor clinical outcome in these patients. Selective inhibition of only the caspase 9-mediated pathway may explain the paradoxical observation that many patients with expression of Bcl-2, XIAP, or both demonstrate high levels of spontaneous apoptosis (Figure 3B-C). Furthermore, it suggests that in these patients, caspase 8-induced activation of caspase 3 does not depend on activation of the caspase 9-mediated pathway through truncation of the proapoptotic Bcl-2 family member Bid<sup>42</sup> (Figure 1).

Combination therapy with rituximab and CHOP has been shown to be more effective than therapy with CHOP alone for treating elderly patients with DLBCL.<sup>43</sup> In addition, it was found that Bcl-2-positive patients benefit especially from this combination therapy,<sup>44</sup> suggesting that rituximab-induced cell death is independent of the caspase 9-mediated pathway and that the apoptosis profile should also predict response to rituximab. This topic is the subject of a new prospective study. Of note, none of the patients studied here had been treated with a rituximab-containing regimen.

Immunohistochemical apoptosis profiles correlated well with our functional analysis of apoptosis sensitivity. In isolated lymphoma cells from a restricted number of patients, we demonstrated that DLBCL patients with caspase 9 inhibition profiles were more resistant to chemotherapy-induced apoptosis than were patients with caspase 8 inhibition profiles (Table 6).

Surprisingly, patients with DLBCL with caspase 9-only inhibition profiles fared significantly worse, especially in the intermediate high/high IPI group, than patients with caspase 8 and caspase 9 inhibition profiles. Our data cannot explain these observations, but they suggest the existence of additional apoptosis-inhibiting factors, such as loss of apoptosis-activating factor-1 (Apaf-1),<sup>45</sup> in patients with chemotherapy-refractory lymphoma with caspase 8 and caspase 9 inhibition profiles. We are investigating the existence of these putative additional factors using microarray expression analysis.

Recently, it has been shown that expression patterns of DLBCL separate GCB from non-GCB DLBCL by mRNA expression profiling and immunohistochemical analysis.<sup>21,23</sup> We were able to confirm the data of Hans et al<sup>23</sup> because our patients with GCB-like DLBCL had significantly better prognoses than those with non-

**Table 7. GCB or non-GCB profile in relation to apoptosis profile**

Apoptosis profile	GCB profile		P*
	GCB n = 25	Non-GCB n = 43	
<b>Caspase 9 inhibition</b>			
No	6	3	.05
Yes	19	40	
<b>Caspase 8 inhibition</b>			
No	8	14	NS
Yes	17	29	

NS indicates not significant.

\*As determined by Fisher exact test. In 12 patients, no material was left to determine GCB profile.

GCB like DLBCL. Interestingly, patients with non-GCB-like profiles more often displayed caspase 9 inhibition profiles ( $P = .05$ ; Table 7), providing a possible explanation for their less favorable prognoses.

This is in accordance with the microarray results of Alizadeh et al,<sup>21</sup> who also identified Bcl-2 and c-Flip among the class-predicting genes between GCB and activated B-cell DLBCL.<sup>46</sup> Only the strong contribution of Bcl-2, but not of c-Flip to the prognostic power of microarray analysis was confirmed in the recent study by Lossos et al.<sup>47</sup> Supervised clustering analysis of microarray expression data by Shipp et al<sup>48</sup> did not identify c-FLIP, Bcl-2, or XIAP as an informative marker but did identify other useful apoptosis-regulating genes. Although microarray analysis is a powerful tool to identify prognostic markers, the clustering algorithms used group genes according to similar expression profiles and as yet do not allow characterization of the functional status of signaling pathways. This limits the comparability of microarray data to our model-based analysis. Future clustering algorithms based on analysis of specific signaling pathways, such as the model published by Fussenegger et al,<sup>49</sup> might identify all involved apoptosis-regulating genes, possibly providing better prediction of response to therapy.

Our observation that some chemotherapy-refractory DLBCLs have an apparently intact caspase 8-mediated pathway can be used to specifically trigger the caspase 8 pathway by TRAIL/Apo2L.<sup>50,51</sup> This strategy has been shown previously to be feasible in therapy-refractory multiple myeloma cells.<sup>52</sup> Thus, TRAIL/Apo2L might offer an alternative treatment for some patients with chemotherapy-resistant DLBCL. Studies determining the sensitivity of DLBCL cells to TRAIL/Apo2L are under way.

We conclude that all patients with primary nodal DLBCL demonstrate immunohistochemical evidence suggestive of caspase 8 and/or caspase 9 inhibition and that a caspase 8 inhibition-only profile predicts a highly favorable clinical outcome whereas a caspase 9 inhibition-only profile strongly predicts poor clinical response to therapy. The possibly intact caspase 8-mediated pathway in some chemotherapy-refractory DLBCL presents an opportunity for treatment with death receptor triggering therapies, including TRAIL/Apo2L.

## Acknowledgments

We thank Prof Dr R. Willemze, Dr L. H. Siegenbeek van Heukelom, Dr M. A. MacKenzie, and Dr. M. J. Flens for their help in collecting clinical data and fresh lymphoma biopsy specimens.

## References

1. A clinical evaluation of the International Lymphoma Study Group classification of non-Hodgkin's lymphoma: the Non-Hodgkin's Lymphoma Classification Project. *Blood*. 1997;89:3909-3918.
2. The International Non-Hodgkin's Lymphomas Prognostic Factors Project. A predictive model for aggressive non-Hodgkin's lymphoma. *N Engl J Med*. 1993;329:987-994.
3. Johnstone RW, Ruefli AA, Lowe SW. Apoptosis: a link between cancer genetics and chemotherapy. *Cell*. 2002;108:153-164.
4. Kitada S, Pedersen IM, Schimmer AD, Reed JC. Dysregulation of apoptosis genes in hematopoietic malignancies. *Oncogene*. 2002;21:3459-3474.
5. Rathmell JC, Thompson CB. The central effectors of cell death in the immune system. *Annu Rev Immunol*. 1999;17:781-828.
6. Schimmer AD, Welsh K, Pinilla C, et al. Small-molecule antagonists of apoptosis suppressor XIAP exhibit broad antitumor activity. *Cancer Cell*. 2004;5:25-35.
7. Thome M, Tschopp J. Regulation of lymphocyte proliferation and death by FLIP. *Nat Rev Immunol*. 2001;1:50-58.
8. Johnstone RW, Ruefli AA, Lowe SW. Apoptosis: a link between cancer genetics and chemotherapy. *Cell*. 2002;108:153-164.
9. Schmitt CA, Lowe SW. Bcl-2 mediates chemoresistance in matched pairs of primary E(mu)-myc lymphomas in vivo. *Blood Cells Mol Dis*. 2001;27:206-216.
10. Kroemer G, Reed JC. Mitochondrial control of cell death. *Nat Med*. 2000;6:513-519.
11. Korsmeyer SJ. BCL-2 gene family and the regulation of programmed cell death. *Cancer Res*. 1999;59:1693s-1700s.
12. Kuppers R, Klein U, Hansmann ML, Rajewsky K. Cellular origin of human B-cell lymphomas. *N Engl J Med*. 1999;341:1520-1529.
13. van Eijk M, Defrance T, Hennino A, de Groot C. Death-receptor contribution to the germinal-center reaction. *Trends Immunol*. 2001;22:677-682.
14. Wang J, Lobito AA, Shen F, Hornung F, Winoto A, Lenardo MJ. Inhibition of Fas-mediated apoptosis by the B cell antigen receptor through c-Flip. *Eur J Immunol*. 2000;30:155-163.
15. Hennino A, Berard M, Casamayor-Palleja M, Krammer PH, Defrance T. Regulation of the Fas death pathway by FLICE-inhibitory protein in primary human B cells. *J Immunol*. 2000;165:3023-3030.
16. Hennino A, Berard M, Krammer PH, Defrance T. FLICE-inhibitory protein is a key regulator of germinal center B cell apoptosis. *J Exp Med*. 2001;193:447-458.
17. van Eijk M, Medema JP, de Groot C. Cutting edge: cellular Fas-associated death domain-like IL-1-converting enzyme-inhibitory protein protects germinal center B cells from apoptosis during germinal center reactions. *J Immunol*. 2001;166:6473-6476.
18. Thomas RK, Kallenborn A, Wickenhauser C, et al. Constitutive expression of c-Flip in Hodgkin and Reed-Sternberg cells. *Am J Pathol*. 2002;160:1521-1528.
19. Mathas S, Lietz A, Anagnostopoulos I, Hummel F, et al. c-FLIP mediates resistance of Hodgkin/Reed-Sternberg cells to death receptor-induced apoptosis. *J Exp Med*. 2004;199:1041-1052.
20. Dukers DF, Oudejans JJ, Vos W, ten Berge RL, Meijer CJ. Apoptosis in B-cell lymphomas and reactive lymphoid tissues always involves activation of caspase 3 as determined by a new in situ detection method. *J Pathol*. 2002;196:307-315.
21. Alizadeh AA, Eisen MB, Davis RE, et al. Distinct types of diffuse large B-cell lymphoma identified by gene expression profiling. *Nature*. 2000;403:503-511.
22. Shipp MA, Ross KN, Tamayo P, et al. Diffuse large B-cell lymphoma outcome prediction by gene-expression profiling and supervised machine learning. *Nat Med*. 2002;8:68-74.
23. Hans CP, Weisenburger DD, Greiner TC, et al. Confirmation of the molecular classification of diffuse large B-cell lymphoma by immunohistochemistry using a tissue microarray. *Blood*. 2004;103:275-282.
24. Jaffe ES, Harris NL, Stein H, Vardiman JW. Pathology and genetics of tumors of haematopoietic and lymphoid tissues: World Health Organisation Classification of Tumors. Lyon, France: IARC Press; 2001.
25. Gospodarowicz MK, Sutcliffe SB. The extranodal lymphomas. *Semin Radiat Oncol*. 1995;4:281-300.
26. Casciola-Rosen L, Nicholson DW, Chong T, et al. Apopain/CPP32 cleaves proteins that are essential for cellular repair: a fundamental principle of apoptotic death. *J Exp Med*. 1996;183:1957-1964.
27. Germain M, Affar EB, D'Amours D, Dixit VM, Salvesen GS, Poirier GG. Cleavage of automodified poly(ADP-ribose) polymerase during apoptosis: evidence for involvement of caspase-7. *J Biol Chem*. 1999;274:28379-28384.
28. Oudejans JJ, Jiwa NM, Kummer JA, et al. Analysis of major histocompatibility complex class I expression on Reed-Sternberg cells in relation to the cytotoxic T-cell response in Epstein-Barr virus-positive and -negative Hodgkin's disease. *Blood*. 1996;87:3844-3851.
29. Oudejans JJ, Jiwa NM, Kummer JA, et al. Activated cytotoxic T cells as prognostic marker in Hodgkin's disease. *Blood*. 1997;89:1376-1382.
30. Cox DR. Regression models and life tables. *J R Stat Soc Br*. 1972;34:187.
31. Armitage JO, Weisenburger DD for the Non-Hodgkin's lymphoma classification project. New approach to classifying non-Hodgkin's lymphomas: clinical features of the major histologic subtypes. *J Clin Oncol*. 1998;16:2780-2795.
32. Krajewski S, Gascoyne RD, Zapata JM, et al. Immunolocalization of the ICE/Ced-3-family protease, CPP32 (caspase-3), in non-Hodgkin's lymphomas, chronic lymphocytic leukemias, and reactive lymph nodes. *Blood*. 1997;89:3817-3825.
33. Chang DW, Xing Z, Pan Y, et al. cFLIP<sub>L</sub> is a dual function regulator for caspase-8 activation and CD95-mediated apoptosis. *EMBO J*. 2002;21:3704-3714.
34. Krueger A, Schmitz I, Baumann S, Krammer PH, Kirchhoff S. Cellular FLICE-inhibitory protein splice variants inhibit different steps of caspase-8 activation at the CD95 death-inducing signaling complex. *J Biol Chem*. 2001;276:20633-20640.
35. Hermine O, Haioun C, Lepage E, et al. Prognostic significance of bcl-2 protein expression in aggressive non-Hodgkin's lymphoma: Groupe d'Etude des Lymphomes de l'Adulte (GELA). *Blood*. 1996;87:265-272.
36. Barrans SL, Carter I, Owen RG, et al. Germinal center phenotype and bcl-2 expression combined with the International Prognostic Index improves patient risk stratification in diffuse large B-cell lymphoma. *Blood*. 2002;99:1136-1143.
37. Kramer MH, Hermans J, Parker J, et al. Clinical significance of Bcl-2 and p53 protein expression in diffuse large B-cell lymphoma: a population-based study. *J Clin Oncol*. 1996;14:2131-2138.
38. Devereaux QL, Takahashi R, Salvesen GS, Reed JC. X-linked IAP is a direct inhibitor of cell-death proteases. *Nature*. 1997;388:300-304.
39. Kashkar H, Haefs C, Shin H, et al. XIAP-mediated caspase inhibition in Hodgkin's lymphoma-derived B cells. *J Exp Med*. 2003;198:341-347.
40. Bratton SB, Lewis J, Butterworth M, Duckett CS, Cohen GM. XIAP inhibition of caspase-3 preserves its association with the Apaf-1 apoptosome and prevents CD95- and Bax-induced apoptosis. *Cell Death Differ*. 2002;9:881-892.
41. Shiozaki EN, Chai J, Rigotti DJ, et al. Mechanism of XIAP-mediated inhibition of caspase-9. *Mol Cell*. 2003;11:519-527.
42. Li H, Zhu H, Xu CJ, Yuan J. Cleavage of BID by caspase 8 mediates the mitochondrial damage in the Fas pathway of apoptosis. *Cell*. 1998;94:491-501.
43. Coiffier B, Lepage E, Briere J, et al. CHOP chemotherapy plus rituximab compared with CHOP alone in elderly patients with diffuse large-B-cell lymphoma. *N Engl J Med*. 2002;346:235-242.
44. Mounier N, Briere J, Gisselbrecht C, et al. Rituximab plus CHOP (R-CHOP) overcomes bcl-2-associated resistance to chemotherapy in elderly patients with diffuse large B-cell lymphoma (DLBCL). *Blood*. 2003;101:4279-4284.
45. de Boer WP, Oudejans JJ, Meijer CJ, Lankelma J. Analysing gene expressions with GRANK. *Bioinformatics*. 2003;19:2000-2001.
46. Davis RE, Brown KD, Siebenlist U, Staudt LM. Constitutive nuclear factor  $\kappa$ B activity is required for survival of activated B cell-like diffuse large B cell lymphoma cells. *J Exp Med*. 2001;194:1861-1874.
47. Lossos IS, Czerwinski DK, Alizadeh AA, et al. Prediction of survival in diffuse large-B-cell lymphoma based on the expression of six genes. *N Engl J Med*. 2004;350:1828-1837.
48. Shipp MA, Ross KN, Tamayo P, et al. Diffuse large B-cell lymphoma outcome prediction by gene-expression profiling and supervised machine learning. *Nat Med*. 2002;8:68-74.
49. Fussenegger M, Bailey JE, Varner J. A mathematical model of caspase function in apoptosis. *Nat Biotechnol*. 2000;18:768-774.
50. Wiley SR, Schooley K, Smolak PJ, et al. Identification and characterization of a new member of the TNF family that induces apoptosis. *Immunity*. 1995;3:673-678.
51. Pitti RM, Marsters SA, Ruppert S, Donahue CJ, Moore A, Ashkenazi A. Induction of apoptosis by Apo-2 ligand, a new member of the tumor necrosis factor cytokine family. *J Biol Chem*. 1996;271:12687-12690.
52. Mitsiades CS, Treon SP, Mitsiades N, et al. TRAIL/Apo2L ligand selectively induces apoptosis and overcomes drug resistance in multiple myeloma: therapeutic applications. *Blood*. 2001;98:795-804.